Influence of inherent anisotropy of soil strength on limit equilibrium slope stability analysis

Brandon Karchewski, Peijun Guo & Dieter Stolle
Department of Civil Engineering – McMaster University, Hamilton, Ontario, Canada

ABSTRACT
Limit equilibrium analysis is a common technique used in geotechnical engineering to arrive at a factor of safety for the stability of a slope. The traditional form of limit equilibrium analysis assumes that the soil strength is homogeneous and isotropic, which is typically not the case in the field. Soil strength depends on factors such as stress level, rate of load application, and soil fabric; the literature often refers to the latter as "inherent" anisotropy. This study examines the influence of inherent anisotropy by incorporating simple strength models that account for the orientation of the sliding plane relative to the bedding plane into the limit equilibrium calculation. Numerical examples from the literature are re-evaluated using the Morgenstern-Price method combined with a genetic algorithm to search for the critical non-circular slip surface considering the effects of inherent anisotropy. The effect on the shape and location of the critical slip surface is negligible. The magnitude of the reduction in factor of safety may be up to 9% for a 15% range of orientation-dependent soil strength.

RÉSUMÉ
L'analyse de l'équilibre limite est une technique couramment utilisée en géotechnique pour obtenir un facteur de sécurité de la stabilité de pente. La forme traditionnelle de l'analyse d'équilibre limite suppose que la résistance du sol soit homogène et isotrope, ce qui n'est pas généralement le cas sur le champ. La résistance du sol dépend de facteurs tels que le niveau de contrainte, le taux d'application de charge, et le tissu du sol; la littérature se réfère souvent à ce dernier comme anisotropie «inhérent». Cette étude examine l'influence de l'anisotropie inhérente en intégrant des modèles de résistance simples qui prend en considération l'orientation du plan de glissement par rapport au plan de stratification dans le calcul d'équilibre limite. Des exemples numériques tirés de la littérature sont réévalués en utilisant la méthode Morgenstern-Price combiné avec un algorithme génétique pour rechercher la surface de rupture critique non-circulaire en tenant compte des effets d'anisotropie inhérente. L'effet sur la forme et l'emplacement de la surface de glissement critique est négligeable. L'ampleur de la réduction de facteur de sécurité peut atteindre 9% pour un domaine de 15% de la résistance du sol dépendant de l'orientation.

1 INTRODUCTION

Slope stability analysis using limit equilibrium methods is common in geotechnical engineering. Limit equilibrium techniques work by selecting a potential slip surface, a priori, dividing the soil mass into a series of slices, and (by making certain assumptions about the interslice forces) computing a factor of safety based on force equilibrium, moment equilibrium, or both. Since one generally does not know the shape or location of the most critical slip surface in advance, limit equilibrium methods require a search algorithm to locate the surface yielding the minimum factor of safety.

Classical limit equilibrium analysis assumes that the strength properties of the soil are isotropic. However, careful analysis of soil properties has shown that the strength of both cohesive and cohesionless soils tend to be anisotropic (e.g. Casagrande and Carillo 1944; Park and Tatsuoka 1994). Anisotropy is related to a number of factors including the magnitude and orientation of applied stresses (Oda et al. 1985) as well as the fabric of the material. The latter is primarily influenced by the orientation of the bedding plane that arises due to the geologic process of sedimentation; anisotropy due to material fabric is often termed inherent anisotropy.

This study focuses on investigating the influence of inherent strength anisotropy on the results of slope stability analysis. The remainder of Section 1 provides a brief literature review on the topics of limit equilibrium analysis, critical slip surface search techniques, and strength models for inherent anisotropy. Section 2 summarizes the specific models and techniques implemented in the code developed for this study. Section 3 presents numerical examples that this study re-examines including a discussion of the poignant results from these examples. Section 4 lists the important conclusions of this research.

1.1 Limit equilibrium analysis

A large number of techniques for analyzing the stability of slopes have been developed over the past century (Duncan, 1996). Each method has its benefits and shortcomings. These have been investigated and summarized in various review papers (Fredlund and Krahn 1977; Duncan and Wright 1980; Duncan 1996). Some of the more popular limit equilibrium methods are the ordinary method of slices (Fellenius 1927), Bishop's modified method (Bishop 1955), Janbu's generalized procedure of slices (Janbu 1968), and the Morgenstern-

Price method (1965). The Morgenstern-Price method is particularly popular since it allows analysis of general shapes of slip surface and variation of the interslice force distribution. Its derivation is relatively rigorous in that it satisfies both force and moment equilibrium on the global and local levels. It is also relatively stable numerically (Duncan 1996). Zhu et al. (2005) developed an efficient algorithm for the Morgenstern-Price method based on a generalised framework for limit equilibrium analysis (Zhu et al. 2003) that typically converges within a few iterations.

1.2 Slip surface optimization

Locating the most critical slip surface is an optimization problem involving a highly nonlinear objective function with many local minima. For this reason, it is difficult to solve using traditional gradient-based root finding techniques. In particular, for the case of a non-circular slip surface, the search for the global minimum has been accomplished by making use of many techniques including Monte Carlo simulation (Greco 1996; Husein Malkawi et al. 2001), dynamic programming (Pham and Fredlund 2003), particle swarm optimization (Cheng et al. 2007), genetic algorithms (Zolfaghari et al. 2005; Li et al. 2010), and other techniques that make use of kinematic and stress field admissibility criteria (Kim et al. 2002; Sarma and Tan 2006).

Direct search techniques such as Monte Carlo simulation or genetic algorithms require problem-specific start-up algorithms and stopping criteria. Boutrup and Lovell (1980) developed a start-up algorithm for slope stability problems that selects entry and exit angles based on the geometry of the slope and Rankine theory, which was successful in their own study and has also been used, albeit slightly modified, in more recent studies (Greco 1996; Li et al. 2010). Cheng et al. (2007) reported success with a set of dual stopping criteria in the context of particle swarm optimization; the search is considered complete only when the change in the factor of safety remains below a specified relative difference for a specified number of iterations. The stopping criterion must be specified in this way to prevent the algorithm from stopping prematurely at a local minimum. Li et al. (2010) applied the same set of stopping criteria for use with a genetic algorithm.

1.3 Inherent anisotropy

Several studies have investigated the effect of inherent anisotropy on the strength of cohesive soils. A few examples are those carried out by Casagrande and Carillo (1944), Lo (1965), and Davis and Christian (1971). Law (1978) used the model proposed by Lo (1965) based on the square of the direction cosine of the principal stress directions to develop an approximate modification factor for the stability of constructed slopes overlying cohesive soils. Graham (1979) investigated the stability of constructed slopes overlying soft cohesive materials including the influence of anisotropy, among other factors, using total stress analysis.

The inherent anisotropy of granular soils has also been investigated both experimentally and numerically. Meyerhof (1978) proposed modifications to bearing capacity analysis to account for anisotropic behaviour of cohesionless materials. Park and Tatsuoka (1994) examined the anisotropic behaviour of sand using plane strain compression tests. Guo and Stolle (2005) as well as Chang and Yin (2010) used micromechanical analysis to evaluate the anisotropic behaviour of granular materials.

Much work has been done on incorporating inherent anisotropy of soils into generalized plasticity models (e.g. Oda 1993; Pietruszczak and Mroz 2001; Abelev and Lade 2004; Dafalias et al. 2004; Gao et al. 2010). For stability analysis, however, it is more desirable to have a simplified functional relationship between the soil fabric and a minimal set of strength parameters along specified directions that can be obtained using standardized tests. For example, as a corollary to micromechanical modelling, Guo (2008) developed a modified procedure for the direct shear test that can be used to obtain the strength of granular materials for various bedding plane orientations relative to the plane being sheared.

2 MODEL

This section outlines the numerical model developed for this study, which has been implemented in Matlab. The model combines limit equilibrium analysis using the Morgenstern-Price method, a genetic algorithm for locating the critical slip surface, and a set of simplified models for anisotropic strength.

2.1 Limit equilibrium

The approach herein uses of a modified form of the algorithm for the Morgenstern-Price method as presented by Zhu et al. (2005) to evaluate the factor of safety. Figure 1 shows the force balance for a slice where F_s is the factor of safety (assumed constant over the entire slip surface), λ is a scalar relating interslice normal force to interslice shear force, f_i is the value of the interslice shear force distribution function, φ_i' is the effective angle of friction for the slice, c_i' is the effective cohesion for the slice, and all other terms are as defined in Table 1 and Table 2. Note that this representation differs from that presented by Zhu et al. (2005) in that interslice water forces are accounted for explicitly and the interslice normal force, E_i', is in terms of effective stress rather than total stress. Note that the water pressure at the surface, U_i^t, is only non-zero if the water surface lies above the top boundary of the slice.

Following Zhu et al. (2005), summing forces along the directions of N_i' and S_i and rearranging to eliminate these terms yields the following recursion relation for the interslice normal forces:

$$E_i'\Phi_i = \Psi_{i-1}E_{i-1}'\Phi_{i-1} + F_s T_i - R_i \qquad [1]$$

where Φ_i and Ψ_{i-1} are defined as:

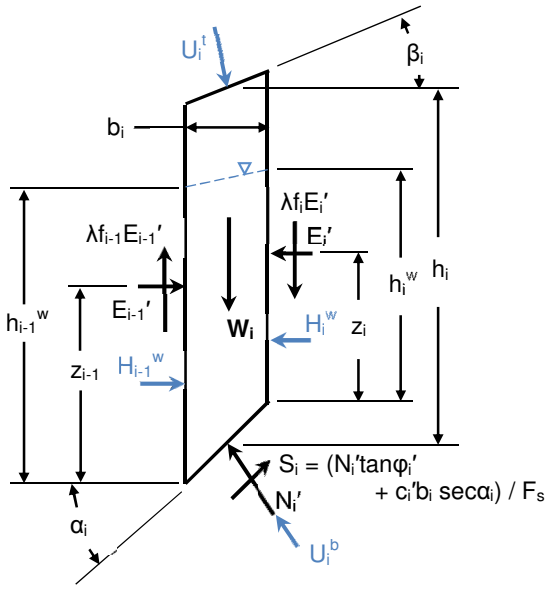

Figure 1. Free-body diagram of a slice

Table 1. Nomenclature for slice diagram (forces)

Parameter	Description
W_i	Weight of slice
N_i'	Effective normal force at base
S_i	Mobilized shear force at base
U_i^b, U_i^t	Force of water pressure (b=bottom, t=top)
E_{i-1}', E_i'	Effective interslice normal forces
$\lambda f_{i-1} E_{i-1}'$, $\lambda f_i E_i'$	Interslice shear forces
H_{i-1}^w, H_i^w	Interslice force due to water pressure

Table 2. Nomenclature for slice diagram (dimensions)

Parameter	Description
b_i	Width of slice
h_i	Height of slice at centreline
z_{i-1}, z_i	Height of interslice normal force
h_{i-1}^w, h_i^w	Height of interslice water pressure force
α_i	Angle of base of slice
β_i	Angle of top of slice

$$\Phi_i = (\lambda f_i \cos\alpha_i - \sin\alpha_i)\tan\varphi_i' - (\lambda f_i \sin\alpha_i - \cos\alpha_i)F_s \quad [2a]$$

$$\Psi_{i-1} = \frac{(\lambda f_{i-1} \cos\alpha_i - \sin\alpha_i)\tan\varphi_i' - (\lambda f_{i-1} \sin\alpha_i - \cos\alpha_i)F_s}{\Phi_{i-1}} \quad [2b]$$

and T_i and R_i represent the mobilized and resisting shear forces at the base, given by:

$$T_i = W_i sin\alpha_i + (H_i^w - H_{i-1}^w)cos\alpha_i + U_i^t(\cos\beta_i \sin\alpha_i - \sin\beta_i \cos\alpha_i) \quad [3a]$$

$$R_i = [(W_i + U_i^t \cos\beta_i)\cos\alpha_i + (U_i^t \sin\beta_i - H_i^w + H_{i-1}^w)\sin\alpha_i]\tan\varphi_i' + c_i' b_i \sec\alpha_i \quad [3b]$$

Summing equation 1 over all slices, assuming that $E_0'=E_n'=H_0^w=H_n^w=0$, yields the following definition for F_s:

$$F_s = \frac{\sum_{i=1}^{n-1} R_i \left(\prod_{j=i}^{n-1} \Psi_j\right) + R_n}{\sum_{i=1}^{n-1} T_i \left(\prod_{j=i}^{n-1} \Psi_j\right) + T_n} \quad [4]$$

where n is the number of slices. Taking moment equilibrium about the centre of the base of the slice and summing over all slices yields the following definition for λ:

$$\lambda = \frac{\sum_{i=1}^{n} [b_i (E_i' + E_{i-1}' + H_i + H_{i-1})\tan\alpha_i - 2h_i U_i^t \sin\beta_i]}{\sum_{i=1}^{n} b_i (f_i E_i' + f_{i-1} E_{i-1}')} \quad [5]$$

In general, a solution is obtained by iteratively updating Φ_i, Ψ_{i-1}, and E_i' until the estimates for F_s and λ converge. The details of the numerical algorithm are as presented by Zhu et al. (2005).

2.2 Genetic algorithm

As mentioned previously, the evaluation of a single slip surface does not constitute a complete solution of a slope stability problem; one must seek the slip surface that minimizes the factor of safety. This is an N-P hard class of problem (Cheng et al. 2007) since the form of the objective function for the factor of safety is highly irregular and depends on a large number of parameters including the coordinates of the slip surface, the slope geometry, the subsurface stratigraphy, and the strength properties of the soil layers. In practice, the minimization process has been achieved with a wide variety of techniques as discussed in the literature review. The analysis herein uses a genetic algorithm as proposed by Li et al. (2010) since it is a relatively efficient search technique for this class of problem. The details are not discussed here since the exposition by Li et al. (2010) is comprehensive, but in broad terms the algorithm proceeds as follows:

(i) Initialize a population of slip surfaces for evaluation with the Morgenstern-Price method using the start-up algorithm proposed by Boutrup and Lovell (1980) based on sensible ranges for entry and exit coordinates and angles. Initially the surfaces are defined by four vertices: the entry and exit points and two interior points. Each surface is divided into 36 slices for evaluation.

(ii) Verify that each surface meets the requirements for kinematic admissibility (Li et al. 2010).

(iii) Evaluate the factor of safety for each slip surface that meets the requirements in step (ii).

(iv) Sort the surfaces from lowest to highest factor of safety and apply a weighting scheme such that surfaces with significantly lower values for factor of safety receive a very high probability density.

(v) Randomly select pairs of parent surfaces and perform crossover (interpolation) to generate new vertex locations based on a set of dynamic bounds for each coordinate.

(vi) Apply random mutation to the newly generated surfaces.

(vii) Repeat steps (ii)-(vi) until the set of convergence criteria proposed by Cheng et al. (2007) are satisfied. On each iteration, check intermediate convergence criteria for adding more vertices to the definition of the slip surfaces.

Note that in the final step, the number of vertices is recursively increased to 2n-1 where n is the current number of vertices. Since the initial number of vertices is 4, this corresponds to the sequence {4,7,13,25,…}. Li et al. (2010) noted that no significant improvement in the solution is achieved by increasing the number of vertices from 13 to 25, so the analysis herein uses a maximum of 13 vertices to define the slip surface. It should be noted that these vertices act as control points for defining the shape of the surface, but the surface is always divided into 36 slices for evaluation.

2.3 Anisotropic strength models

This section aims to show that incorporating the effects of inherent anisotropy into the framework for slope stability analysis set out in the previous sections is relatively straightforward provided one has appropriate relationships for the cohesive and frictional strength of the material that can be determined from the geometry of the slope and a minimal set of characteristic strengths. The models in this section use the naming convention for angles shown in Figure 2. The bedding plane angle, θ, defines the direction of the soil fabric, which arises due to sedimentation. The angle α is the angle between the sliding plane and the horizontal; this corresponds to the angle at the base of a slice in limit equilibrium analysis. The angle δ gives the orientation of the principal stresses relative to the normal to the bedding plane and the angle ξ gives the orientation of the sliding plane relative to the bedding plane. Note that the principal stress directions are assumed to be at 45°+φ′/2 from the sliding plane. The consequence of this assumption is that the model is applicable only for low levels of anisotropy since, strictly

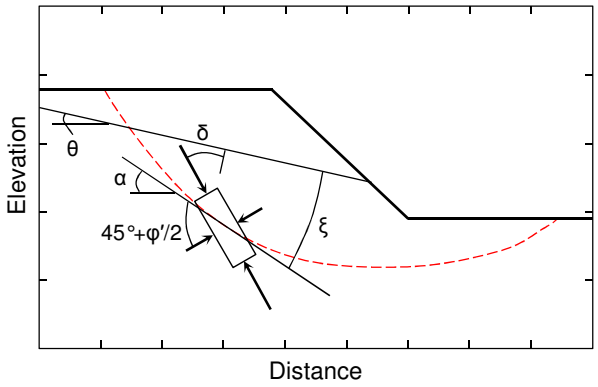

Figure 2. Angle definitions for anisotropic models

speaking, the failure plane angle of 45°+φ′/2 only applies to isotropic materials.

The analysis herein uses the model for inherent anisotropy of strength in cohesive soils proposed by Lo (1965):

$$c' = c'_{=} + (c'_{\perp} - c'_{=})\cos^2\delta \qquad [6]$$

where $c_{=}'$ and $c_{\perp}'$ are the effective cohesive strengths when the major principal stress is applied parallel (δ=90°) and perpendicular (δ=0°) to the bedding plane, respectively. Defining the degree of anisotropy, $k_c = c_{=}'/c_{\perp}'$, equation 6 may also be written as:

$$c' = c_{\perp}'[k_c + (1 - k_c)\cos^2\delta] \qquad [7]$$

which allows the minimum cohesive strength to be more easily specified as some proportion of the maximum cohesion value. Assuming that the sliding plane makes an angle of 45°+φ′/2 with the major principal stress, the angle δ is given by:

$$\delta = 45° + \varphi'/2 - \mathrm{abs}(\alpha) + \theta\,\mathrm{sgn}(\alpha) \qquad [8]$$

where the absolute value function, abs(), and the sign function, sgn(), have been used to account for the change in orientation of the principal stresses as α changes sign.

While the cohesive strength model above has existed for almost half a century, a similar functional relationship for frictional strength has proven more elusive. The analysis herein uses a simplified model developed on the basis of micromechanical analysis by Guo and Stolle (2005):

$$\tan\varphi' = \mu_0[1 - \varpi\cos(2\xi)] \qquad [9]$$

where the parameters μ_0 and ϖ are given by:

$$\mu_0 = \tfrac{1}{2}(\tan\varphi_{\perp}' + \tan\varphi_{=}') \quad [10a]$$

$$\varpi = \frac{\tan\varphi_{\perp}' - \tan\varphi_{=}'}{\tan\varphi_{\perp}' + \tan\varphi_{=}'} \quad [10b]$$

where $\varphi_{=}'$ and $\varphi_{\perp}'$ are the angles of friction for sliding parallel (ξ=0°) and perpendicular (ξ=90°) to the bedding plane, respectively.

Although at a glance the cohesive strength and frictional strength seem to be related to different orientation angles, by substituting equation 8 into equation 7 the angle δ may be obtained in terms of ξ as:

$$\delta = 45° + \tfrac{1}{2}\text{atan}(\mu_0[1 - \varpi cos(2\xi)]) - \text{abs}(\alpha) + \theta\,\text{sgn}(\alpha) \quad [11]$$

Since ξ is a function of only α and θ, it is clear that δ and ξ are not independent parameters. Using the relation in equation 11, one may rewrite equation 7 in terms of ξ or vice versa for equation 9 and δ. However, for convenience, the presented forms are used with φ' being computed first since it is required to compute δ.

The anisotropic models presented above compute cohesive and frictional strength based only on a limited set of strength parameters, the geometry of the slip surface, and the angle of the bedding plane associated with the stratigraphy. Thus inherent anisotropy is incorporated into the slope stability analysis framework by modifying the computation of the strength at the base of each slice. The additional input requirements compared with analysis assuming isotropic soil strength are the specification of strength values in two directions (as opposed to one arbitrary direction) and the angle of the bedding plane for each stratigraphic layer.

3 NUMERICAL EXAMPLES

This section analyzes a series of example problems to demonstrate the influence of inherent anisotropy on the factor of safety. Each example has been previously analyzed by multiple researchers for isotropic strength conditions. In each case, the results from the present model for isotropic conditions are shown for verification. Subsequently, each example is examined considering anisotropy of cohesive and frictional strength separately and jointly.

3.1 Example 1

The first example is a slope of homogeneous cohesive-frictional material. Figure 3 shows the geometry of the slope, which has a gradient of 0.5 (β≈26.6°). The unit weight of the material is 17.64 kN/m^3. The anisotropic cohesive strength parameters are $c_{\perp}'$=9.80 kPa and $c_{=}'$=8.33 kPa, where $c_{\perp}'$ corresponds to the isotropic strength value used by past researchers (Greco 1996; Husein Malkawi 2001; Cheng et al. 2007; Li et al. 2010); the selected minimum strength value gives the slope a degree of anisotropy of 0.85. The frictional strength parameters are $\varphi_{\perp}'$=10° and $\varphi_{=}'$=8.5°, where $\varphi_{\perp}'$ is the isotropic strength value used by past researchers. The bedding plane angle is θ=0° for the results shown in Figure 3.

The result for the isotropic case shows good agreement (relative difference ≤ 1.5%) with the results of Greco (1996), Cheng et al. (2007) and Li et al. (2010). There is a discrepancy with the result reported by Husein Malkawi et al. (2001), however, as noted by Cheng et al. (2007) this result is questionable. Cheng et al. (2007) re-evaluated the slip surface reported by Husein Malkawi et al. (2001) to obtain F_s=1.370; re-analysis with the implementation of the Morgenstern-Price method used in the present study yields F_s=1.352.

It is clear from the results that strength anisotropy has negligible influence on the shape and location of the slip surface. This result has been noted in the past by Al-

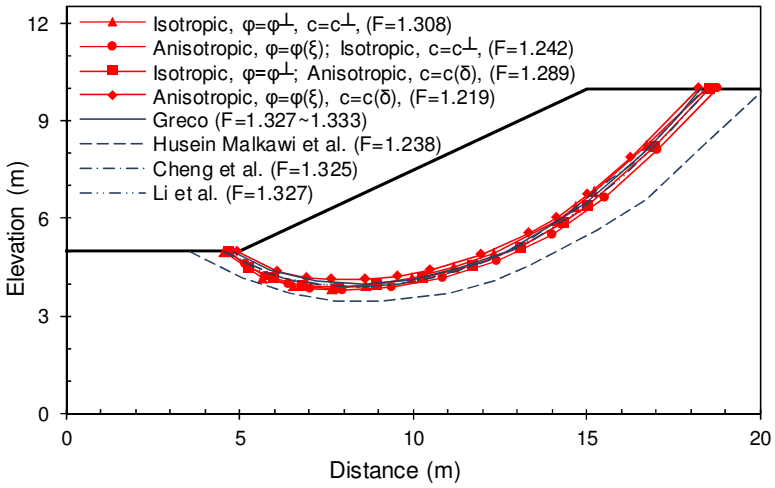

Figure 3. Results of analysis for Example 1

Karni and Al-Shamrani (2000), albeit for circular slip surfaces and variation of cohesive strength only. The results presented herein make an even stronger statement about the influence of strength anisotropy on the shape and location of the slip surface since the shape is left as a variable in the present analysis and variation of frictional strength is also considered. Since strength anisotropy does not influence the shape or location of the slip surface, one could uncouple these portions of the analysis for practical purposes. Note, however, that this statement may only be applicable to the low levels of anisotropy for which this model is applicable.

The results show that the factor of safety is reduced by 5.0%, 1.5% and 6.8% considering anisotropy of cohesive strength, frictional strength and both, respectively. These values may seem relatively small, however, these results are for deterministic material properties. Since the strength properties of material in the field are subject to uncertainty, one should consider the result in the context of probabilistic analysis such as the framework proposed by El-Ramly et al. (2002). In such context, small decreases in the factor of safety can lead to a larger number of cases where the factor of safety is less than unity and thus a higher probability of failure.

Since this example considers a slope of homogeneous material, it is also interesting to examine the variation in the factor of safety for various bedding plane angles. As shown above, the shape and location of the critical slip surface are not influenced by strength anisotropy. Thus, only the critical surface obtained for the isotropic strength values is re-evaluated in this phase of the analysis. Figure 4 shows the results for various bedding plane angles with the resulting factors of safety normalized to the value obtained for isotropic conditions (F_{max}=1.308). It is evident that the bedding plane angle resulting in the minimum factor of safety is not the same for anisotropy of cohesive and frictional strength. Note that the bedding plane angle resulting in the minimum factor of safety considering anisotropy of frictional strength only is approximately this makes sense intuitively since it means that the slope is

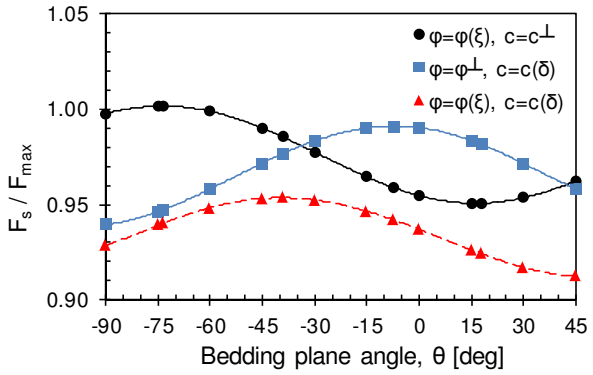

Figure 4. Variation of F_s with θ for Example 1

weakest when the bedding plane is parallel to the average sliding direction of the failing soil mass. Similarly, the greatest factor of safety for variation in frictional strength occurs when the bedding plane is perpendicular to the average sliding direction ($\theta_{max} \approx$ atan(-1/tan(mean(α)) ≈ -73.7°). The maximum reduction in factor of safety is 8.8% for a degree of anisotropy, k_c, of 0.85.

3.2 Example 2

Figure 5 shows the stratigraphy of the second example. This slope consists of three layers of material, one of which is a thin layer of weak frictional material. The presence of a water table is also indicated. Table 3 shows the material properties for the layers with the layer number increasing with depth. The values taken for the maximum strength coincide with the isotropic material properties used in previous studies.

The results for isotropic analysis agree within a relative difference of 1.5% with the results of Pham and Fredlund (2003) for dynamic programming analysis and the results of Li et al. (2010) using a genetic algorithm (both using the Morgenstern-Price method to evaluate F_s).

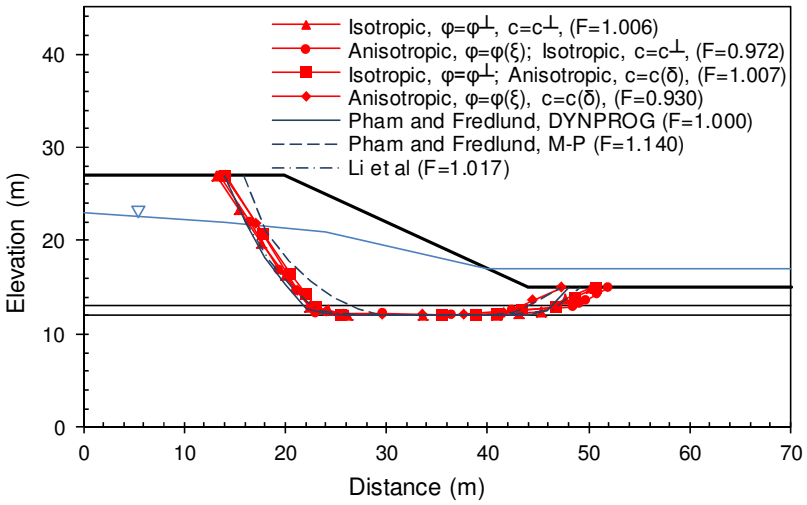

Figure 5. Results of analysis for Example 2

Table 3. Material properties for Example 2

Layer	$\varphi_{\perp}'$ [deg]	$\varphi_{=}'$ [deg]	$c_{\perp}'$ [kPa]	$c_{=}'$ [kPa]	γ [kN/m^3]	γ_{sat} [kN/m^3]
1	30.0	25.5	20.0	17.0	15.0	15.0
2	10.0	8.5	0.0	0.0	18.0	18.0
3	30.0	25.5	100.0	85.0	20.0	20.0
Water					9.8	

There is a discrepancy with the second result reported by Pham and Fredlund (2003), but it should be noted that this was not obtained through a true non-circular analysis, but rather the surface was defined by a composite circular-linear shape. As one would expect, the thin, weak layer controls the failure mechanism; the factor of safety is nearly unity, which means that this case is incipient on failure for isotropic strength conditions.

Considering anisotropy of cohesive and frictional strength separately, it is clear that the frictional strength has a stronger influence. The reduction in the factor of safety is 3.4% when considering anisotropy of frictional strength alone. The factor of safety obtained when considering anisotropy of cohesive strength alone is apparently larger than that obtained for isotropic conditions by 0.1%. This is explained by the probabilistic nature of the minimization process with a genetic algorithm; if a larger number of analyses were carried out for the cohesive strength anisotropy case, one would eventually obtain a lower value for F_s, however for the present purpose the difference is considered negligible. The fact that frictional strength anisotropy is important while the influence of cohesive strength anisotropy is negligible in this case is explained by the fact that the failure mechanism is controlled by a thin layer that possesses only frictional strength. Considering the anisotropy of both strength components simultaneously, a 7.6% reduction in the factor of safety is obtained. This magnification of the influence of the anisotropy may be related to the fact that frictional strength and cohesive strength have different correlations with the bedding plane angle as shown in Figure 4. More research into the coupled effect of these two strength components is required before drawing this conclusion.

It is worth repeating in this particular example a point that was raised in the discussion of example 1. Note that the slope has $F_s \approx 1.0$ for isotropic strength conditions. When the influence of strength anisotropy is considered, F_s reduces to below unity indicating that the slope is unstable. In the context of a probabilistic analysis where the strength properties and the geometry of the problem become random variables (El-Ramly et al. 2002), a larger number of such cases may occur possibly leading to a significantly higher probability of failure.

4 CONCLUSIONS

The analysis herein has successfully incorporated anisotropy of cohesive and frictional strength into the framework of limit equilibrium analysis of non-circular slip surfaces. The following conclusions are noted:

- Strength anisotropy can be quite readily integrated into limit equilibrium analysis provided that appropriate models for anisotropic strength are available; the models used herein have been taken from the literature on strength anisotropy, but once could just as easily use a custom model based on empirical data if desired.
- Low levels of strength anisotropy have negligible influence on the shape and location of the slip surface; this implies that the analysis for the location of the critical surface and the influence of strength anisotropy may be uncoupled for practical purposes.
- Considering frictional strength anisotropy, the factor of safety is minimized when the bedding plane angle is coincident with the average base angle of the critical surface (i.e. the average sliding direction); conversely, the factor of safety is maximized when the bedding plane angle is perpendicular to the average sliding direction of the soil mass.
- The variation of factor of safety with respect to bedding plane angle for anisotropy of cohesive and frictional strength components is different; more research is required into the appropriateness of combining anisotropic models for these components of strength.
- Consideration of strength anisotropy leads to reductions in the factor of safety on the order of 5~10% for a degree of anisotropy of 0.85. The difference may seem small, but when incorporated into a more complete probabilistic analysis, such a reduction in the factor of safety may lead to a significantly higher probability of failure. An important next step in this research will be the incorporation of the present model into such a probabilistic analysis.

ACKNOWLEDGEMENTS

The authors would like to acknowledge the Natural Sciences and Engineering Research Council of Canada (NSERC) and the Department of Civil Engineering at McMaster University for financial support of this work.

REFERENCES

Abelev, A.V. and Lade, P.V. 2004. Characterization of failure in cross-anisotropic soils, *Journal of Engineering Mechanics*, 130(5): 599-606.

Al-Karni, A.A. and Al-Shamrani, M.A. 2000. Study of the effect of soil anisotropy on slope stability using method of slices, *Computers and Geotechnics*, 26(2): 83-103.

Bishop, A.W. 1955. The use of the slip circle in the stability analysis of slopes, *Géotechnique*, 5(1): 7-17.

Boutrup, E. and Lovell, C. 1980. Searching techniques in slope stability analysis, *Engineering Geology*, 16(1-2): 51-61.

Casagrande, A. and Carillo, N. 1944. Shear failure of anisotropic soils, *Journal of the Boston Society of Civil Engineers*, 32(2): 74-87.

Chang, C.S. and Yin, Z.Y. 2010. Micromechanical modeling for inherent anisotropy in granular materials, *Journal of Engineering Mechanics*, 136(7): 830-839.

Cheng, Y., Li, L., Chi, S. and Wei, W. 2007. Particle swarm optimization algorithm for the location of the critical non-circular failure surface in two-dimensional slope stability analysis, *Computers and Geotechnics*, 32(2): 92-103.

Dafalias, Y., Papadimitriou, A. and Li, X. 2004. Sand plasticity model accounting for inherent fabric anisotropy, *Journal of Engineering Mechanics*, ASCE, 130(11): 1319-1334.

Davis, D. and Christian, J. 1971. Bearing capacity of anisotropic cohesive soils, *Journal of the Soil Mechanics and Foundations Division*, ASCE, 97(SM5): 753-769.

Duncan, J. 1996. State of the art: limit equilibrium and finite-element analysis of slopes, *Journal of Geotechnical Engineering*, ASCE, 122(7): 577-596.

El-Ramly, H., Morgenstern, N. and Cruden, D. 2002. Probabilistic slope stability analysis for practice, *Canadian Geotechnical Journal*, 39(3): 665-683.

Fellenius, W. 1927. *Erdstatische Berechnungen mit Reibung und Kohasion*, Ernst, Berlin (in German).

Fredlund, D. and Krahn, J. 1977. Comparison of slope stability methods of analysis, *Canadian Geotechnical Journal*, 14(3): 429-439.

Gao, Z., Zhao, J. and Yao, Y. 2010. A generalized anisotropic failure criterion for geomaterials, *International Journal of Solids and Structures*, 47(22-23): 3166-3185.

Graham, J. 1979. Embankment stability on anisotropic soft clays, *Canadian Geotechnical Journal*, 16(2): 295-308.

Greco, V. 1996. Efficient Monte Carlo technique for locating critical slip surface, *Journal of Geotechnical Engineering*, ASCE, 122(7): 517-525.

Guo, P. 2008. Modified direct shear test for anisotropic strength of sand, *Journal of Geotechnical and Geoenvironmental Engineering*, ASCE, 134(9): 1311-1318.

Guo, P. and Stolle, D. 2005. On the failure of granular materials with fabric effects, *Soils and Foundations*, 45(4): 1-12.

Husein Malkawi, A., Hassan, W. and Sarma, S. 2001. Global search method for locating general slip surface using Monte Carlo techniques, *Journal of Geotechnical and Geoenvironmental Engineering*, ASCE, 127(8): 688-698.

Janbu, N. 1968. Slope stability computations, *Soil Mechanics and Foundation Engineering Report*, The Technical University of Norway, Trondheim, Norway.

Kim, J., Salgado, R. and Lee, J. 2002. Stability analysis of complex soil slopes using limit analysis, *Journal of Geotechnical and Geoenvironmental Engineering*, ASCE, 128(7): 546-557.

Law, K. 1978. Undrained strength anisotropy in embankment stability, *Canadian Geotechnical Journal*, 15(2): 306-309.

Li, Y., Chen, Y., Zhan, T., Ling, D. and Cleall, P. 2010. An efficient approach for locating the critical slip surface in slope stability analyses using a real-coded genetic algorithm, *Canadian Geotechnical Journal*, 47(7): 806-820.

Lo, K. 1965. Stability of slopes in anisotropic soils, *Journal of the Soil Mechanics and Foundations Division*, ASCE, 91(SM4): 85-106.

Morgenstern, N. and Price, V. 1965. The analysis of the stability of general slip surfaces, *Géotechnique*, 15(1): 79-93.

Oda, M. 1993. Inherent and induced anisotropy in plasticity theory of granular soils, *Mechanics of Materials*, 16(1-2): 35-45.

Oda, M., Nemat-Nasser, S. and Konishi, J. 1985. Stress-induced anisotropy in granular masses, *Soils and Foundations*, 25(3): 85-97.

Park, C. and Tatsuoka, F. 1994. Anisotropic strength and deformations of sands in plane strain compression, *Proceedings of the Thirteenth International Conference on Soil Mechanics and Foundation Engineering*, New Delhi, India, 1: 1-4.

Pham, H. and Fredlund, D. 2003. The application of dynamic programming to slope stability analysis, *Canadian Geotechnical Journal*, 40(4): 830-847.

Pietruszczak, S. and Mroz, Z. 2001. On failure criteria for anisotropic cohesive-frictional materials, *International Journal for Numerical and Analytical Methods in Geomechanics*, 25(5): 509-524.

Sarma, S. and Tan, D. 2006. Determination of critical slip surface in slope analysis, *Géotechnique*, 56(8): 539-550.

Zhu, D., Lee, C. and Jiang, H. 2003. Generalised framework of limit equilibrium methods for slope stability analysis, *Géotechnique*, 53(4): 377-395.

Zhu, D., Lee, C., Qian, Q. and Chen, G. 2005. A concise algorithm for computing the factor of safety using the Morgenstern-Price method, *Canadian Geotechnical Journal*, 42(1): 272-278.

Zolfaghari, A., Heath, A. and McCombie, P. 2005. Simple genetic algorithm search for critical non-circular failure surface in slope stability analysis, *Computers and Geotechnics*, 32(3): 139-152.